RESEARCH ARTICLE

Editorial Process: Submission:04/05/2024 Acceptance:08/30/2024

In Vivo Detection of Multidrug-Resistance Related Proteins in Locally Advanced Breast Cancer Using ^{99m}Tc-MIBI SPECT/CT Imaging: Correlation with Clinical Outcomes

Nadia M Mostafa[1], Maha S Elnaggar[1], Yasser G Abdelhafez[2,3], Khalid Rezk[4], Mahmoud Farouk Sherif[5], Hanan A Eltyb[6], Shaimaa Ahmed[2], Nagm Eldin Abu Elnga[7], Marwa T Hussien[8]*

Abstract

Objective: Neoadjuvant chemotherapy (NACT) is widely used for treating locally advanced Breast cancer (LABC). However, development of multidrug resistance (MDR) is the main underlying factor for chemoresistance. Technetium-^{99m} methoxyisobutylisonitrile (^{99m}Tc-MIBI) is a substrate for MDR. This study aimed to analyze the relationship between expression of MDR-related proteins (P-gp and Bcl-2) and ^{99m}Tc-MIBI uptake and retention in BC tumor cells, pathologic response to NACT, disease free survival (DFS) and overall survival (OS). **Methods:** prospective analysis recruited 31 patients with LABC who received NACT between January 2019 and March 2020. ^{99m}Tc-MIBI planar and SPECT/CT imaging was conducted before and after NACT. Qualitative and quantitative analyses were performed, pre and post-NACT early and delayed lesion to non-lesion (LNL) ratios, and retention index (RI) of ^{99m}Tc-MIBI were calculated. Expression of P-gp and Bcl-2 in tumor cells was determined by immunohistochemistry. **Results:** Quantitively, inter-reader ICC for SPECT/CT based quantification was consistently higher than that of planar images. Post-NACT LNL ratios were significantly higher in patients with pathologic persistent disease (PPD). A change in RI between pre- and post-NACT scans demonstrated a significant association with DFS with a hazard ratio of 0.7 (95%CI: 06-1.0). Qualitatively, SPECT/CT was significantly more accurate compared to planar imaging in identifying residual viable tumor (81% compared to 57%). Her2neu positivity and high post-operative Bcl-2 and P-gp were associated with worse DFS. A significant association was found between increased expression of post-NACT Bcl-2 and PPD, advanced tumor stage and poor OS. **Conclusion:** ^{99m}Tc-MIBI SPECT/CT based qualitative evaluation of BC response to NACT is more accurate than planar imaging. Post-NACT MIBI retention is positively correlated with P-gp and Bcl-2 expression. ^{99m}Tc-MIBI SPECT/CT may predict MDR development. High post-NACT Bcl-2 expression is significantly associated with advanced tumor stage and OS. High post-NACT P-gp expression has a worse impact on pathologic response and DFS.

Keywords: Breast cancer- ^{99m}Tc-MIBI SPECT/CT- Bcl2- Pgp- survival

Asian Pac J Cancer Prev, **25 (9)**, 3125-3141

Introduction

Breast cancer (BC) is the most frequently diagnosed cancer among women and the leading cause of cancer mortality worldwide, with 2.3 million new cases and 685,000 deaths in 2020 [1]. Locally advanced BC (LABC) includes bulky primary breast tumors (large tumors or those involving the skin or chest wall) and BC with extensive lymphadenopathy, as defined by the American Joint Committee on Cancer (AJCC) staging system [2] Worldwide, approximately 20-25% of BC patients have LABC at presentation, yet this percentage is significantly less in countries with implemented screening programs [3]

Despite the fact that there are several different methods of cancer therapies, including radiotherapy, immunotherapy, surgery, hormonal therapy, and gene therapy, albeit chemotherapy still remains the key method for cancer management [4] Neoadjuvant chemotherapy (NACT) employing anthracycline-based chemotherapies is used in BC for the treatment of

*[1]Department of Clinical Oncology and Nuclear Medicine, Faculty of Medicine, Assiut University, Egypt. [2]Department of Radiation Oncology and Nuclear Medicine, South Egypt cancer institute, Assuit University, Egypt. [3]Department of Radiology, University of California Davis, Sacramento, CA, U S A. [4]Department of Surgical Oncology, South Egypt cancer institute, Assuit University, Egypt. [5]Department of Pathology, Faculty of medicine, Assuit University, Egypt. [6]Department of Medical Oncology and Malignant Hematology, South Egypt cancer institute, Assuit University, Egypt. [7]General Surgery Department, Faculty of Medicine, Assiut University, Egypt. [8]Department of Oncologic Pathology, South Egypt Cancer Institute, Assiut University, Egypt. *For Correspondence: marwat.hussien@aun.edu.eg*

inoperable and locally advanced disease. Different studies have shown that neoadjuvant treatment increases the possibility of breast-conserving surgery [5]. However, up to 90% of treatment failures in cancer are attributed to chemoresistance [6].

The ability of cancer cells to become simultaneously resistant to several structurally unrelated chemotherapeutic agents with different mechanisms of action is referred to as multidrug resistance (MDR). Currently, MDR remains a major obstacle to successful chemotherapy, causing progression or relapse of most malignant tumors. Moreover, once MDR develops, the treatment options are very limited, and the possibility of a cure is almost non-existent [7]. Generally, drug resistance could be innate or acquired; innate resistance is when MDR is naturally expressed in cancer cells, while acquired resistance is due to gaining mutation(s) during the process of carcinogenesis [8]. The underlying mechanisms in the development of the two phenotypes of MDR are multiple, different, and complex. One of the important and well understood MDR mechanisms is an ATP-dependent increased anti-cancer drug efflux attributed to the over expression of certain members of the ATP-binding cassette (ABC) membrane transporter superfamily [9]. Among members of this superfamily, P-glycoprotein (P-gp, ABCB1), MDR-associated protein 1 (MRP1, ABCC1), and BC resistance protein (BCRP, ABCG2), are the major players in development of MDR in tumor cells [10]. P-gp transmembrane protein is encoded by the *MDR-1* gene and is the most studied and well-characterized membrane transporter protein associated with resistance to cancer chemotherapy [11]. It functions as a unidirectional efflux transporter for a wide range of xenobiotics and endotoxins via an ATP-dependent mechanism [12]. In the same way, a broad range of hydrophobic chemotherapeutics including anthracyclines, taxanes, epipodophyllotoxins, and vinca alkaloids are substrates for P-gp [9]. A review of a published meta-analysis of 31 studies with more than 1,200 participants demonstrated that P-gp expression is detected in a significant (41%) percentage of BCs [13]. Additional mechanisms of cell resistance, mainly involving defective apoptosis. In particular, overexpression of the anti-apoptotic protein, Bcl-2 on the mitochondrial membrane which protects tumor cells from induction of apoptosis by many different chemotherapeutics [10].

Technetium-^{99m} 2-methoxyisobutylisonitrile (^{99m}Tc-MIBI), a lipophilic radiopharmaceutical that possesses a cationic charge [14], has been previously documented to be a transport substrate for P-gp in a variety of tumor cells [15]. Since it can be actively pumped out of cells with P-gp overexpression, it has been used as an in vivo surrogate marker for P-gp expression [16], Bcl-2 may also affect ^{99m}Tc-MIBI uptake by cancer cells and inhibit tracer accumulation in mitochondria [10]. So, absent or reduced early ^{99m}Tc-MIBI uptake in BC likely reflects the presence of defective apoptosis, while enhanced tracer washout from ^{99m}Tc-MIBI positive lesions likely reflects an overexpression of membrane transporters such as P-gp [17]. A reduction in the apoptotic index and pronounced overexpression of Bcl-2 were found in BC cells which failed to accumulate MIBI [18].

Though multiple previous reports have investigated the relationship between ^{99m}Tc-MIBI uptake and the expression of either P-gp or Bcl-2, and treatment outcomes in LABC [19-22], yet both proteins have not been studied simultaneously. Moreover, most of these studies are based on planar imaging. In this study, we aimed to evaluate the utility of ^{99m}Tc-MIBI SPECT/CT imaging in the functional characterization of MDR related proteins (both P-gp and Bcl-2) in patients with LABC and to correlate the imaging findings with the immunohistochemical analysis of these two proteins. The secondary objective was to assess changes of ^{99m}Tc-MIBI uptake within the tumor and the expression of these proteins after NACT, and to correlate these changes with the clinical outcomes.

Materials and Methods

Patients

This prospective study was approved by the Institutional Committee of Medical Ethics, written informed consent was obtained for all patients. Between January 2019 and March 2020, a total of 34 women with untreated LABC; including large sized operable (stage IIB, IIIA) tumors, inoperable (stage IIIB, IIIC) tumors, as well as inflammatory BC were referred for ^{99m}Tc-MIBI imaging; were initially enrolled in the present study. Patients with evidence of systemic metastases (n=1), non-available paraffin blocks of the pathology specimens for analysis (n=1), and those with poor left ventricular function (n=1) were excluded, leaving a valid cohort of 31 women who were analyzed in this study (Figure 1). The included patients were ≥18 years old and had performance status ≤ 2 according to Eastern Cooperative Oncology Group (ECOG) performance scale [23].

All patients underwent pre-NACT ^{99m}Tc-MIBI imaging within one week from starting NACT. For 21 out of 27 patients who underwent radical/conservative breast surgery, ^{99m}Tc-MIBI scan was repeated after the end of chemotherapy (post-NACT). Expression of P-gp and Bcl-2 was analyzed at two settings: from tru-cut needle biopsies obtained at initial diagnosis and after radical/conservative breast surgery for patients who underwent surgery. Disease-free survival (DFS) and overall survival (OS) were calculated form the date of diagnosis of BC until date of documented recurrence/death or censoring at the last follow-up.

Pre-treatment evaluation

All patients underwent thorough evaluation as a baseline, which included history and clinical examination, complete laboratory investigations to ensure adequate organ and bone marrow function, bilateral breast sonomamagraphy, CT chest and abdomen, ^{99m}Tc-MDP bone scans, and tumor clip-marking. Breast MRI was performed in selected patients who initially were amenable to conservative surgery.

NACT protocol

NACT protocol involved anthracycline with cyclophosphamide followed by taxanes (AC-Taxanes) in the following regimen: Doxorubicin 60 mg/m2 IV plus

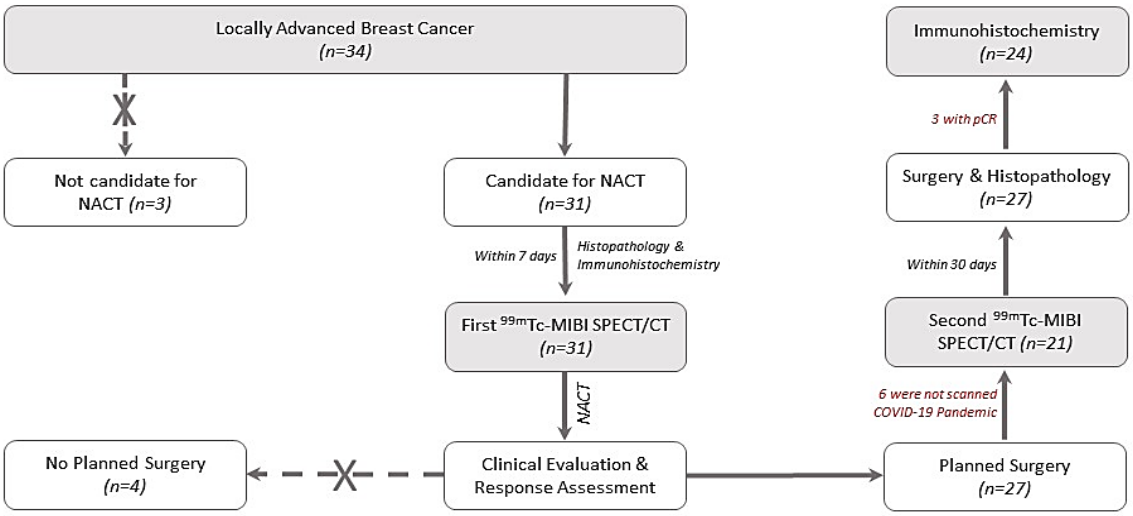

Figure 1. Study Flowchart

cyclophosphamide 600 mg/m^2 IV on day 1, every 3 weeks for four cycles. This was followed by a taxanes; either docetaxel 75 mg/m^2 IV every 3 weeks for four cycles, or paclitaxel 80 mg/m2 IV weekly for 12 weeks. One year of adjuvant trastuzumab was added for patients with HER2 positive disease.

Clinical assessment of response

Regular size assessment was performed by both clinical examination on cycle-by-cycle basis and breast ultrasound every two cycles to guide discontinuation of therapy in a patient with a growing or non-responding tumor and to decide when maximal response of grossly evident disease has been achieved. Mammogram and breast ultrasound were performed prior to surgery, while MRI was selectively obtained in patients who had MR at their initial tumor staging to facilitate comparison. Response to NACT was classified according to the response evaluation criteria in solid tumors (RECIST) [24]. A maximum of two target lesions were assessed inlcuding the longest diameter of the tumor mass(s) and measurbale lymph node (with a short axis more than 1.5 cm). Accordingly, response was classified as complete response, partial response with at least 30% decrease in the longest dimension of the target lesion(s), progressive disease showing at least 20% increase in the longest dimension of target lesion(s), or a stable disease showing no significant change.

The choice of surgical procedure is dependent both on pretreatment disease stage and on its response to NACT; either conservative oncoplastic breast surgery or radical surgery.

Immunohistochemistry

For all cases, the stained hematoxylin and eosin slides were reviewed histologically by pathologist. Formalin-fixed paraffin-embedded (FFPE) tissue blocks were cut to 3-4 μm thick sections and mounted on positively charged slides. The sections were de-paraffinzed and rehydrated in alchol with gradual concentration in decreasing manner. High PH (9) Tris EDTA was used for antigen retrieval in a heated water bath at 90 °C for 45 minutes. A hydrogen peroxide block was applied for 10 min. Two primary antibodies were applied into two separate sections from tumor tissues: primary rabbit monoclonal anti-P Glycoprotein/CD243 antibody (Catalog # YMA1077, Chongqing Biopspes Co., Ltd, China) and a primary rabbit polyclonal anti-Bcl-2 antibody (Catalog # YPA1386, Chongqing Biopspes Co., Ltd, China). The former antibody was used at a dilution of 1/50 and the latter was used at a dilution of 1/150 (optimum dilution according to the data sheet). The tissue sections were then incubated in a humid chamber for 1 hour at room temperature. The universal staining that we applied was a Poly HRP Conjugate, (Ready-To-Use) (Sakura Finetek, USA, 81080825) following the manufacturer's instructions at room temperature for 10 minutes. Streptavidin was applied for 10 minutes, and diaminobenzidine (DAB) solution was then applied to the slides for 5 minutes. A counterstain for the tissue sections was performed using Mayer's hematoxylin. Normal hepatic tissue and reactive lymph node tissues were used as a positive control for P-gp and Bcl-2, respectively.

Evaluation of P-gp and Bcl-2 expression

An unequivocal membraneous brownish staining with or without cytoplasmic staining of P-gp is considered positive. Semiquantitative method were used for evaluation of P-gp expression which depend on the sum of proportion and intensity scores. The proportion score calculated by QuPath V0.4.4 program as the pecentage of positive cells: negative staining, 1–24% of tumor cells were positive, 25–50% were positive and >50% of tumor cells were positive which corresponded to 0, 1, 2 and 3 proportion scores, respectively. Intensity of P-gp staining was evaluated as no staining, weak, moderate and strong which corresponded to 0, 1, 2 and 3 intensity scores [25].

A cytoplasmic brownish staining of Bcl-2 is considered positive. Bcl-2 was evaluated using also the semiquantitative method but with different proportion score. The poportion score ranged from 0 to 5 which presented as: negative, 1%, 2–10 %, 11–30 %, 31–60 %,

>60 % of positive tumor cells for Bcl-2, respectively [26].

P-gp and Bcl-2 scores were applied on pre- and post-NACT specimens. The total score was subdivided into high and low expression with cutoff 3 and 6 for P-gp and Bcl-2 score, respectively.

Positive staining in the bile canaliculi of P-gp and positive staining of Bcl-2 in interfollicular lymphocytes were used as positive controls. Sections of the tissue-specific positive controls were stained using the same protocol but omitting the primary antibody, which was used as a negative control.

^{99m}Tc-MIBI planar and SPECT/CT imaging

Planar ^{99m}Tc-MIBI scans were performed after intravenous injection of 714-919 MBq (19.3-24.8 mCi) of ^{99m}Tc-MIBI in the arm contralateral to the lesion. Early images were acquired 10-30 minutes whereas delayed images were acquired 100-140 minutes after tracer injection. The patient was placed in the prone position on a special breast scintigraphy mattress with cutouts for the breasts to be freely hanging and a shielding pallet in between the two breasts. Images were acquired in the lateral projection with 10-min preset time and 256x256 matrix, with the arms above the head and axillae included in the field of view. Acquisition was performed using a hybrid SPECT/CT dual head gamma camera (Symbia T; Siemens Healthcare, Erlangen, Germany) equipped with low-energy, high resolution collimators, using a 15% energy window centered on the ^{99m}Tc 140 KeV photopeak.

Immediately after planar scintigraphy, with the patient still in the same prone position, SPECT/CT acquisition was obtained in a step-and-shoot mode (25s⁄stop), with 320 frames/head using a noncircular orbit, over 360o arc (180o per head). Then, a low-dose CT scan, for attenuation correction and anatomical localization was acquired with a peak tube voltage of 130 kV, tube current of 80 mA, and dynamic dose reduction algorithm (CARE Dose 4D; Siemens Health care). SPECT images were reconstructed using iterative reconstruction algorithm (Flash3D; Siemens Healthcare, Erlangen, Germany) with 4 iterations, 4 subsets, and 8-mm Gaussian filter. Low-dose CT was used for attenuation correction. Transverse, sagittal, and coronal slices were generated. CT images were reconstructed with slice thickness of 1mm. Finally, SPECT images were hardware coregistered and fused with CT images.

Planar and SPECT image analysis

For both pre- and post-NACT planar/SPECT ^{99m}Tc-MIBI studies, firstly, the images were qualitatively evaluated to detect the site of abnormal tracer uptake (primary tumor site) in the pre-NACT examination as well as the post-NACT studies with residual tracer uptake or the corresponding site of previous positive uptake in the post-NACT studies with no visual evidence of residual lesion.

Volume of interest (VOIs) were delineated independently by two nuclear medicine physicians (reader 1 and 2) with 18 and 19 years of experience, respectively. For planar imaging, VOIs were drawn over the primary tumor on the lateral views, then copied to the corresponding site (background) in the contralateral breast. The maximum count on the lesion and mean count from the contralateral side (non-lesion) were recorded.

For SPECT images, VOIs were drawn under CT guidance in SPECT tranaxial views then copied to the corresponding site in the contralateral breast. Lesion-to-non-lesion (LNL) ratios were calculated by dividing the counts derived from the diseased side to the counts from the VOI delineated on the contralateral or normal breast tissue.

Retention index (RI) was expressed as a percentage calculated for each metric as:

(Early LNL - Delayed LNL) x 100 ÷ Early LNL

Furthermore, the changes in LNL between pre- and post-NACT was calculated separately for the early and delayed LNL, and for RI. Changes were expressed as a percentage as follows:

Change in early LNL ratio = (Early pre-NACT LNL ratio - Early post-NACT LNL ratio) x 100 ÷ Early pre-NACT LNL ratio

Change in delayed LNL ratio = (Delayed pre-NACT LNL ratio - Delayed post-NACT LNL ratio) x 100 ÷ Delayed pre-NACT LNL ratio

Change in RI = pre-NACT RI (%) - post-NACT RI (%)

Post-NACT ^{99m}Tc-MIBI qualitative evaluation

Following the scoring system described by Brem et al. [27], the visual analysis of tracer uptake on the post-NACT ^{99m}Tc-MIBI imaging was scored as: score 1 (no uptake), score 2 (minimal patchy uptake), score 3 (minimal patchy with some areas of more focal uptake), score 4 (abnormal mild focal uptake), and score 5 (abnormal marked focal uptake). For binary analysis, scores 1-3 were considered negative for residual primary tumor, and scores 4-5 were classified as positive for residual tumor.

Qualitative evaluations were acquired during a separate session from quantitative evaluations and were performed independently by the same two experienced nuclear medicine physicians who were blinded to clinical and pathological information except primary tumor side and pre-NACT images. Any discrepancies were resolved by consensus after mutual discussion. All analyses were obtained on a reading workstation running iMac computer (Apple, California, USA) and OsiriX MD (Pixmeo SARL, Bernex, Switzerland).

Statistical analysis

Quantitative data were summarized as mean ± SD and median (range). Qualitative data were summarized as frequencies (number) and relative frequencies (percentages), as appropriate. Association between clinicopathologic characteristics and pre- and post-NACT B-cl2 was performed using chi square or Fisher's exact test, as appropriate.

Inter-reader agreement on categorizing lesions as negative (scores 1-3) or positive (scores 4-5) was performed using kappa analysis. McNemar's test was used to test the differences in sensitivity and specificity between planar and SPECT/CT in detecting residual

tumor in respect to the histopathology as the reference standard. Quantitative metrics from planar and SPECT imaging were not normally distributed and a cubic transformation approach was performed first. Intraclass correlation coefficient (ICC) was used to measure the agreement between the ^{99m}Tc-MIBI quantitative LNL metrics derived by the two readers. Spearman's rank correlation was used to measure the association between ^{99m}Tc-MIBI quantitative LNL metrics and other ordinal or continuous clinico-pathologic characteristics.

Time-to-event analysis was performed using univariate Cox-proportional hazard analysis and the hazard ratio (HR) together with its 95% confidence interval (95%CI) were reported. The time was calculated from date of BC diagnosis till documented date of recurrence (disease-free survival) or death (overall survival) or censoring at the last follow-up. No multivariable analysis was performed due to sample size limitation.

Results

Patients' characteristics

The current study included 31 BC female patients. The mean age was 46±12 years old. Twenty-six patients (84%) were diagnosed histopathologically as invasive duct carcinoma (IDC). Twenty-seven out of thirty-one patients (87%) were deemed operable; of them, 18 (58%) underwent modified radical mastectomy (MRM) and 9 (29%) had conservative breast surgery. Only three patients attained complete pathological response based on Millar grade.

The clinicopathologic characteristics of patients are summarized in Table 1.

Association between clinicopathologic parameters and pre- and post-NACT Bcl-2

According to molecular subtyping of BC, high post-NACT B-cl2 was significantly associated with Luminal A and Her2 enriched type while low expression was significantly associated with triple negative BC (TNBC) (Table 2).

Regarding response status to NACT, pathologic persistence disease (PPD) by Millar grading and MD Anderson residual cancer burden (MDA RCB) was significantly associated with high expression post-NACT Bcl-2 (p= 0.003) and (p= 0.008), respectively. Pre-NACT Bcl-2 high expression scores exhibited significant association with advanced lymph node metastasis (LNM), (P=0.026). Post-NACT Bcl-2 high expression was significantly associated with advanced tumor (P=0.004) and nodal (P=0.011) stages. Post-NACT Bcl-2 high expression showed significant relation with the presence of lymphovascular invasion (LVI), (P=0.006).

Association between clinicopathologic parameters and pre- and post-NACT P-gp

PPD by Millar grading was significantly associated with high expression of post-NACT P-gp (P=0.001) (Table 3). Pre-NACT and Post-NACT P-gp high expression scores exhibited significant association with advanced LNM (P=0.025) and (P=0.006), respectively. Post-NACT P-gp high expression showed significant relation with the presence of LVI (P=0.005).

It is worth noting that post-NACT Bcl-2 and P-gp

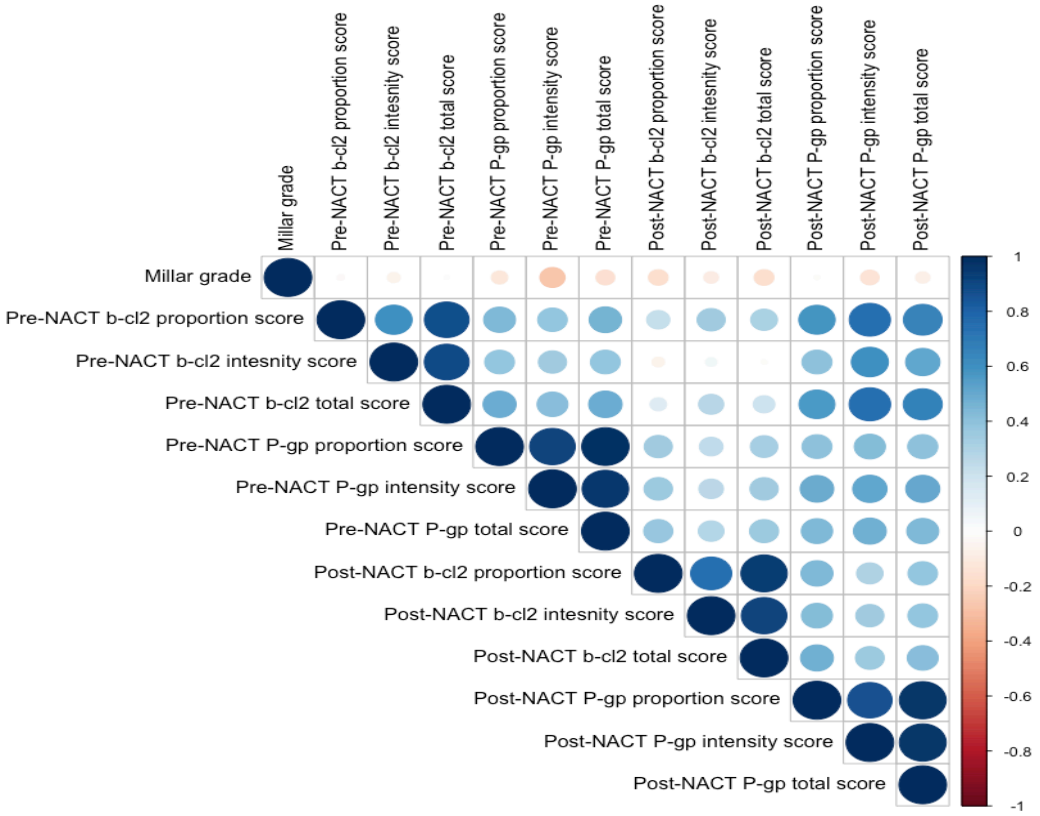

Figure 2. Correlation of Millar Grade of Pathologic Response and pre-/post-NACT Immunohistochemistry Scores

Table 1. Clinicopathologic Characteristics of Patients

Variables	N (%)
Age[a]	
Mean ±SD	46±12.1 (23-69)
<50	18(58%)
≥50	13(42%)
Type of surgery	
MRM	18 (58%)
Conservative	9 (29%)
Not Done	4 (13%)
Tumor Variant	
IDC	26 (84%)
Other Variants	5 (16%)
Tumor side	
Right	21 (68%)
Left	10 (32%)
NACT	
Anthracycline	12 (39%)
Taxanes	3 (9%)
Combined	16 (52%)
ypT	
0	4 (13%)
1	5 (16%)
2	8 (26%)
3	9 (29%)
N/A	5 (16%)
ypN	
0	6 (19%)
1	8 (26%)
2	2 (7%)
3	11 (37%)
N/A	4 (13%)
ER	
Negative	16 (52%)
Positive	11 (36%)
N/A	4 (13%)
PR	
Negative	14 (45%)
Positive	13 (42%)
N/A	4 (13%)
Her2	
Negative	4 (13%)
Positive	21 (68%)
N/A	16 (19%)
Molecular Classification	
Luminal A	9 (29%)
Luminal B	10 (32%)
Her2 Enriched	2 (7%)
Triple Negative	6 (19%)
N/A	4 (13%)
LVI	
No	9 (29%)
Yes	20 (65%)
N/A	2 (7%)
PNI	
No	16 (52%)
Yes	13 (42%)
N/A	2 (6%)
Tumor grade	
G1	1 (3%)
G2	21 (68%)
G3	7 (23%)
N/A	2 (6%)
Millar grade	
pPD	19 (61%)
pPR	6 (19%)
pCR	3 (10%)
N/A	3 (10%)
MDA RCB	
pPD	19 (61%)
pPR	1 (3%)
pCR	4 (13%)
N/A	7 (23%)
Clinical response	
PR	16 (52%)
SD	7 (23%)
CR	5 (16%)
PD	3 (9%)
Ki67a	45.4±31 (5-90)
Time to Progression (months) [a,b]	25.3±11.8 (5.1-44.7)
Time to Death (months) [a,b]	31.3±8.3 (7.1-45.7)

[a], values are given as mean ±SD (min-max); [b], all times are calculated from the date of diagnosis till date of progression/death or censoring at the last follow-up; LVI, Lymphovascular invasion, Perineural invasion; N/A, Non applicable; RBC, residual cancer burden; PR, Partial disease; SD, Stationary disease; CR, Complete response; PD, Persistent disease.

were not associated with the NACT type. Additionally, pre-NACT P-gp and Bcl-2 scores demonstrated substantial positive correlation with post-NACT P-gp scores and overall scores (rho > 0.5, P < 0.05); however, post-NACT Bcl-2 was not significantly associated with any pre-NACT marker (Figure 2).

Planar/SPECT based parameters and their association with Bcl-2 and P-gp

Quantitatively, inter-reader ICC for SPECT/CT quantification was consistently higher than that of planar images. Overall, ICC for different SPECT/CT metrics ranged from 0.67 to 0.89 (Figure 3).

Pre-NACT SPECT/CT metrics were not significantly associated with Bcl-2 or P-gp expression status. However,

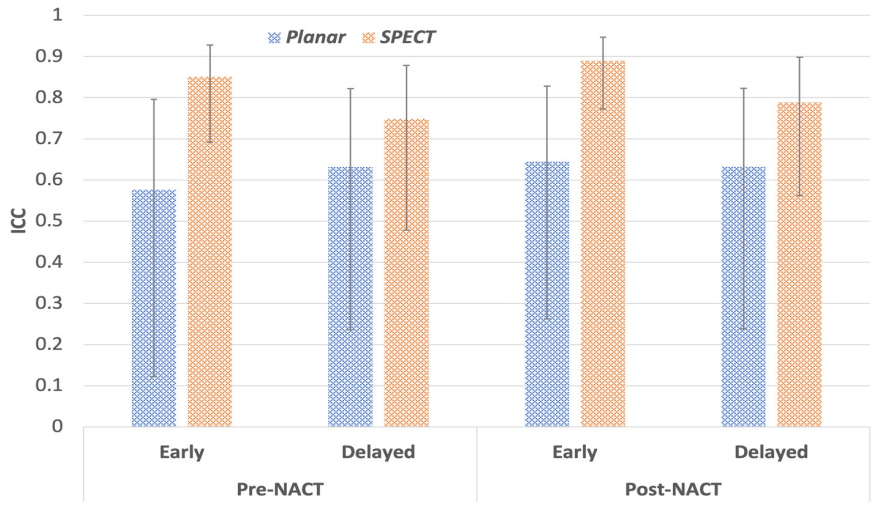

Figure 3. Intraclass Correlation Coefficient for Lesion-Non-Lesion Ratio from Planar and SPECT Images. Error bars represent the 95% confidence interval.

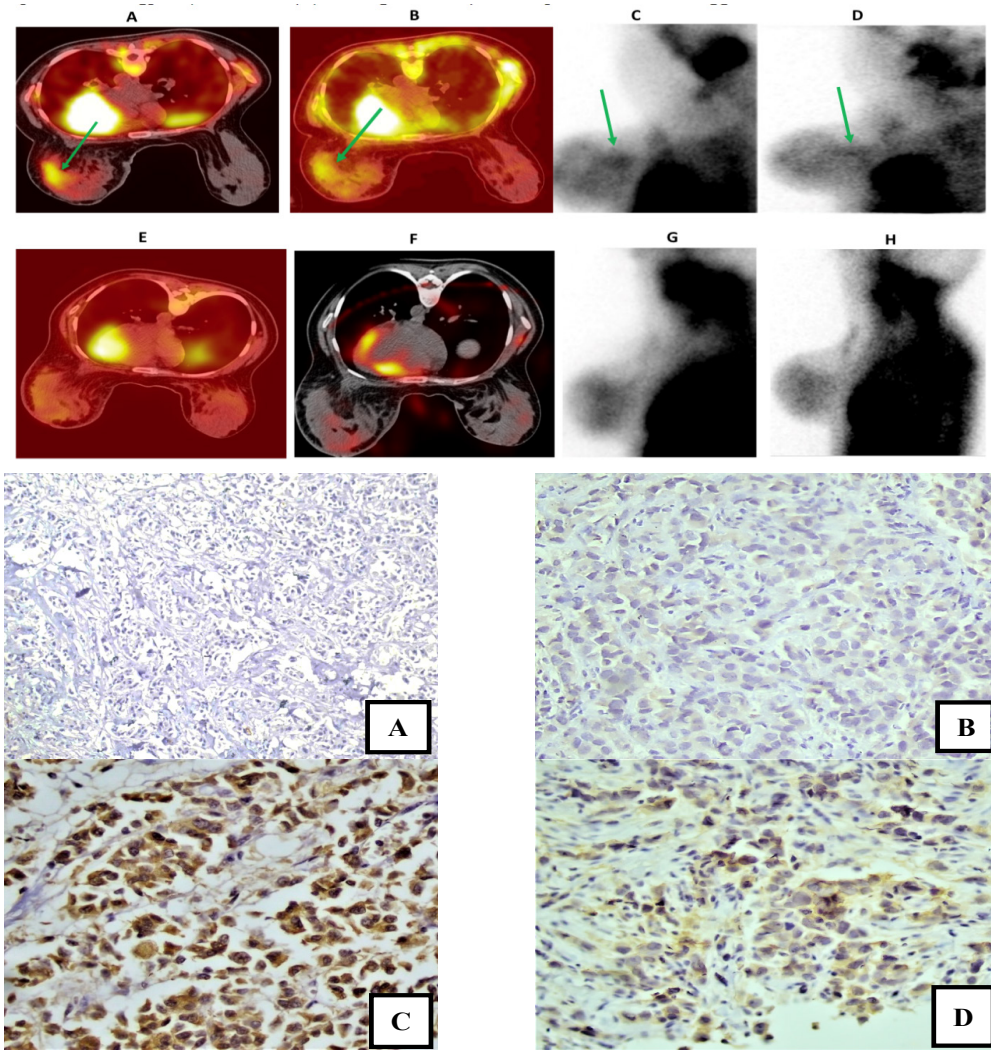

Figure 4. Pre- and post-NACT Early and Delayed 99mTc-MIBI SPECT/CT and Planar Images of 33-Year-Old Women with Left Sided LABC (A, B, C, D) and (E, F, G, H) respectively. Pre-NACT images (Top row) showed positive tracer uptake in tumor (green arrows), with no evidence of metabolically active residual tumor in the post-NACT images (Bottom row) suggesting a good response to NACT. However, post-surgical pathological analysis revealed a persistent pathological disease, denoting a false negative result. Pre- (A&B) and post- NACT (C&D) immunohistochemical profiling of Bcl-2 and P-gp revealed: (A) Pre-NACT cytoplasmic negative expression of Bcl-2 (total score 0) (20X magnification). (B) Pre-NACT cytoplasmic low expression of P-gp (total score 2) (40x magnification). (C) Post-NACT cytoplasmic high expression of Bcl-2 (total score 7) (40x magnification). (D) Post-NACT cytoplasmic high expression of P-gp in (total score 4) (40x magnification). Acquired MDR was suggested.

Table 2. Association between Clinicopathologic Characteristics and Pre- and Post-NACT B-cl2

Characteristics	Pre-NACT B-cl2			#Post-NACT B-cl2		
	Low (n=11)	High (n=20)	P value	Low (n=11)	High (n=13)	P Value
Age						
<50	5 (27.8)	13 (72.2)	0.449	5 (27.8)	8 (44.4)	0.902
≥50	6 (46.2)	7 (53.8)		6 (46.2)	5 (38.5)	
Tumor side						
Right	7 (33.3)	14 (66.7)	1	8 (38.1)	7 (33.3)	0.697
Left	4 (40.0)	6 (60.0)		3 (30.0)	3 (60.0)	
Tumor Variant						
IDC	8 (30.8)	18 (69.2)	0.317	9 (34.6)	10 (38.5)	0.697
Other Variants	3 (60.0)	2 (40.0)		2 (40.0)	3 (60.0)	
ER						
Negative	3 (27.3)	8 (72.7)	0.678	4 (36.4)	3 (27.3)	0.25
Positive	6 (37.5)	10 (63.5)		6 (37.5)	8 (50.0)	
PR						
Negative	3 (23.1)	10 (76.9)	0.503	6 (46.2)	5 (38.5)	1
Positive	6 (42.9)	8 (57.1)		4 (28.5)	6 (42.9)	
Her2						
Negative	8 (38.1)	13 (61.9)	1	9 (42.9)	7 (33.3)	1
Positive	1 (25.0)	3 (75.0)		0 (0)	3 (75.0)	
Molecular Classification						
Luminal A	5 (55.6)	4 (44.4)	0.468	0 (0)	9 (100)	0.008*
Luminal B	2 (20.0)	8 (80.0)		0 (0)	7 (70)	
Her2 Enriched	0 (0)	2 (100)		0 (0)	2 (100)	
Triple Negative	2 (33.3)	4 (66.7)		3 (50)	1 (16.7)	
LVI						
No	5 (55.6)	4 (44.4)	0.312	4 (44.4)	1 (11.1)	0.006*
Yes	6 (30.0)	14 (70.0)		7 (35.0)	11 (55.0)	
PNI						
No	5 (38.5)	8 (61.6)	0.732	5 (38.5)	7 (43.8)	0.568
Yes	6 (37.5)	10 (62.5)		6 (37.)	7 (43.8)	
Tumor grade						
G1	1 (100)	0 (0)	0.588	1 (100)	0 (0)	0.047
G2	8 (38.1)	13 (61.9)		8 (38.1)	10 (47.6)	
G3	2 (28.6)	5 (71.4)		2 (28.6)	2 (28.6)	
NACT						
Anthracycline	4 (33.3)	8 (66.7)	0.648	6 (50.0)	5 (41.7)	0.546
Taxanes	2 (66.7)	1 (33.3)		1 (33.3)	2 (66.7)	
Combined	5 (31.2)	11 (68.8)		4 (25.0)	6 (37.5)	
Type of surgery						
MRM	7 (38.6)	11 (61.1)	0.37	6 (33.3)	11 (61.1)	0.001*
Conservative	4 (44.4)	5 (55.6)		5 (55.6)	1 (11.1)	
ypT						
0	2 (50.0)	2 (50.0)	0.836	1 (25.0)	0 (0)	0.004*
1	1 (20.0)	4 (80.0)		4 (80.0)	0 (0)	
2	3 (37.5)	5 (62.5)		3 (37.5)	5 (62.0)	
3	4 (44.4)	5 (55.6)		3 (33.3)	6 (66.7)	

, data was not available in up to 7 patients: 4 patients did not undergo surgery and 3 had pCR; values are given as number (percentage); pPD, pathologic persistent disease; pPR, pathologic partial response; pCR, pathologic complete response; N/A, not available.

Table 2. Continued

Characteristics	Pre-NACT B-cl2			#Post-NACT B-cl2		
	Low (n=11)	High (n=20)	P value	Low (n=11)	High (n=13)	P Value
ypN						
0	3 (50.0)	3 (50.0)	0.026*	2 (33.0)	0 (0)	0.011*
1	6 (75.0)	2 (25.0)		5 (61.5)	3 (37.5)	
2	0 (0)	2 (100)		1 (50.0)	1 (50.0)	
3	2 (18.2)	9 (81.8)		3 (27.3)	8 (72.7)	
Millar grade						
pPD	7 (36.8)	12 (63.2)	0.647	7 (36.8)	11 (57.90)	0.003*
pPR	3 (50.0)	3 (50.0)		4 (66.7)	1 (16.7)	
pCR	1 (33.3)	2 (66.7)		0 (0)	0 (0)	
MDA RCB						
pPD	6 (31.6)	13 (68.4)	0.649	6 (31.6)	12 (63.2)	0.008*
pPR	1 (100)	0 (0)		1 (100)	0 (0)	
pCR	1 (25.0)	3 (75.0)		1 (25.0)	0 (0)	

, data was not available in up to 7 patients: 4 patients did not undergo surgery and 3 had pCR; values are given as number (percentage); pPD, pathologic persistent disease; pPR, pathologic partial response; pCR, pathologic complete response; N/A, not available.

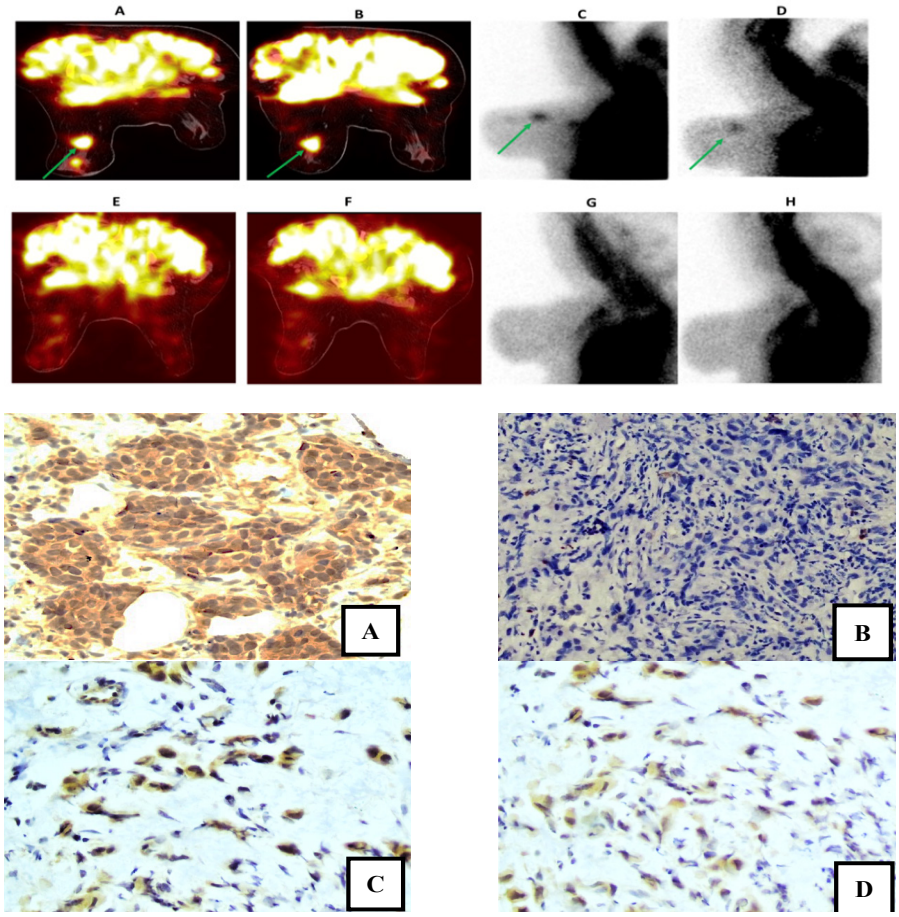

Figure 5. Pre- and Post-NACT Early and Delayed 99mTc-MIBI SPECT/CT and Planar Images of 50-Year-Old Women with Left Sided LABC (A, B, C, D) and (E, F, G, H) respectively. Pre-NACT images (Top row) showed positive tracer uptake in tumor (green arrows), with no evidence of metabolically active residual tumor in the post-NACT images (Bottom row)] suggesting a good response to NACT. However, post-surgical pathological analysis revealed a persistent pathological disease, denoting a false negative result. Pre- (A&B) and post- NACT (C&D) immunohistochemical profiling of Bcl-2 and P-gp revealed: (A) Pre-NACT cytoplasmic low expression of Bcl-2 (total score 5) (40x magnification). (B) Pre-NACT cytoplasmic negative expression of P-gp (total score 0) (20x magnification). (C) Post-NACT cytoplasmic low expression of Bcl-2 (total score 4) (40x magnification). (D) Post-NACT cytoplasmic low expression of P-gp (total score 3) (40x magnification). Surgery was delayed for 50 and 53 days after the end of NACT and 99mTc-MIBI imaging, respectively. Disease progression during this time interval was suggested.]

Table 3. Association between Clinicopathologic Characteristics and Pre and Post-NACT P-gp

Characteristics	Pre-NACT P-gp			#Post-NACT P-gp		
	Low (n=21)	High (n=10)	P value	Low (n=16)	High (n=8)	P Value
Age						
<50	12 (66.7)	6 (33.3)	1	8 (44.4)	6 (33.3)	0.704
≥50	9 (69.2)	4 (30.8)		8 (61.5)	3 (23.1)	
Tumor side						
Right	14 (66.7)	7 (33.3)	1	10 (47.6)	6 (28.6)	0.778
Left	7 (70.0)	3 (30.0)		6 (60.0)	3 (30.0)	
Tumor Variant						
IDC	17 (65.4)	9 (34.6)	1	12 (46.2)	7 (26.9)	0.551
Other Variants	4 (80.0)	1 (20.0)		4 (80.0)	1 (20.0)	
ER						
Negative	7 (63.6)	4 (36.4)	1	5 (45.5)	2 (18.2)	0.35
Positive	11 (68.8)	5 (31.2)		9 (56.2)	6 (50.0)	
PR						
Negative	8 (61.5)	4 (28.6)	0.871	6 (46.2)	5 (38.5)	0.915
Positive	10 (71.4)	4 (28.6)		8 (57.1)	3 (21.4)	
Her2						
Negative	14 (66.7)	7 (33.3)	0.525	12 (57.0)	6 (28.8)	0.774
Positive	2 (50.0)	2 (50.0)		1 (25.0)	2 (50.0)	
Molecular Classification						
Luminal A	5 (55.6)	4 (44.4)	0.234	8 (88.9)	1 (11.1)	0.121
Luminal B	8 (80.0)	2 (20.0)		2 (20.0)	5 (50.0)	
Her2 Enriched	0 (0)	2 (100)		1 (50.0)	1 (50.0)	
Triple Negative	5 (83.3)	1 (16.7)		3 (50.0)	1 (16.7)	
LVI						
No	8 (88.9)	1 (11.1)	0.28	5 (55.6)	0 (0)	0.005*
Yes	12 (60.0)	8 (40.0)		11 (55)	8 (40)	
PNI						
No	9 (68.8)	4 (30.8)	1	6 (46.2)	4 (30.8)	0.422
Yes	11 (68.2)	5 (31.2)		10 (62.5)	3 (18.8)	
Tumor grade						
G1	1 (100)	0 (0)	1	1 (100)	0 (0)	0.137
G2	14 (66.7)	7 (33.3)		13 (61.9)	6 (28.6)	
G3	5 (71.4)	2 (28.6)		2 (28.6)	2 (28.6)	
NACT						
Anthracycline	8 (66.7)	4 (33.3)	1	7 (58.3)	3 (25.0)	0.629
Taxanes	2 (66.7)	1(33.3)		2 (60.7)	1 (33.3)	
Combined	11 (68.8)	5 (31.2)		7 (43.8)	4 (25.0)	
Type of surgery						
MRM	12 (66.7)	6 (33.3)	0.561	12 (66.7)	6 (33.3)	0.003*
Conservative	7 (77.8)	2 (22.2)		4 (44.4)	2 (22.2)	
ypT						
0	3 (75.0)	1 (25.0)	0.45	1 (25.0)	0 (0)	0.117
1	3 (60.0)	2 (40.0)		3 (60.0)	1 (20.0)	
2	5 (62.5)	3 (37.5)		5 (62.5)	3 (37.5)	
3	8 (88.9)	1 (11.1)		5 (55.6)	4 (44.4)	

data was not available in up to 7 patients: 4 patients did not undergo surgery and 3 had pCR; values are given as number (percentage); pPD, pathologic persistent disease; pPR, pathologic partial response; pCR, pathologic complete response. N/A, not available.

Table 3. Continued

Characteristics	Pre-NACT P-gp			#Post-NACT P-gp		
	Low (n=21)	High (n=10)	P value	Low (n=16)	High (n=8)	P Value
ypN						
0	5(83.3)	1(16.7)	0.025*	3(50.0)	0(0)	0.006*
1	8(100.0)	0(0)		6(75.0)	2(25.0)	
2	0(0)	2(100)		1(50.0)	1(50.0)	
3	6(54.5)	5(45.5)		6(54.5)	5(45.5)	
Millar grade						
pPD	13(68.4)	6(31.6)	1	11(57.9)	7(36.8)	0.001*
pPR	4(66.7)	2(33.3)		5(83.3)	1(16.7)	
pCR	2(66.7)	1(33.3)		0(0)	0(0)	
MDA RCB						
pPD	12(63.2)	7(36.8)	0.636	11(57.9)	7(63.8)	0.056
pPR	1(100)	0(0)		1(100)	0(0)	
pCR	2(50.0)	2(50.0)		1(25.0)	0(0)	

data was not available in up to 7 patients: 4 patients did not undergo surgery and 3 had pCR; values are given as number (percentage); pPD, pathologic persistent disease; pPR, pathologic partial response; pCR, pathologic complete response. N/A, not available.

RI tended to demonstrate a significant negative correlation with pre-NACT Bcl-2 intensity scores (rho= -0.364) (Table 4).

Post-NACT SPECT/CT qualitative scores demonstrated significant inverse correlation with post-NACT P-gp proportion scores (rho = -0.474; P = 0.04). Additionally, post-NACT SPECT/CT early LNL ratios tended to demonstrate negative correlation with Bcl-2 overall and P-gp proportion scores; (rho = -0.394, P = 0.09) and (rho = -0.406, P = 0.08), respectively. Furthermore, RI was negatively correlated with P-gp intensity scores (rho = -0.425, P = 0.07) (Table 4).

It is worth noting that post-NACT LNL were significantly higher in patients who did not attain complete pathological response compared to those with pCR (Supplement Table S1).

Qualitatively, inter-reader agreement on categorizing lesions as negative or positive was slightly higher for SPECT/CT (kappa = 0.57; 95%CI: 0.26-0.87) compared to planar images (kappa = 0.36; 95%CI: -0.02-0.75). Overall, SPECT/CT was significantly more accurate compared to planar imaging in identifying residual viable tumor (81% compared to 57%). SPECT/CT demonstrated residual disease in 5 of 8 false negative scans on planar imaging with marginally higher sensitivity (P=0.07) (Supplement Table S2 and S3).

Features associated with progression and overall survival

After a median follow-up of 31.5 months (7.1 - 45.7 months), 12 patients progressed, and 12 patients died (including nine of the twelve who progressed), with 3-year DFS of 58.6% and 3-year OS of 63%.

On univariate analysis (Table 5), her2neu positivity and higher post-NACT Bcl-2 and P-gp scores were associated with worse DFS. Some other clinical characteristics tended to demonstrate association with progression, including (age < 50 yrs, ypT, ypN).

Only PNI and higher post-NACT Bcl-2 scores were significantly associated with poor OS. ypN and PR+ were marginally associated with survival.

Among SPECT/CT imaging metrics, only the change in RI between pre- and post-NACT scans demonstrated significant association with DFS (Table 5) with a hazard ratio of 0.7 (95%CI: 06-1.0).

Table 4. Spearman's Correlation Coefficient between SPECT based Metrics and B-cl2 & P-gp Scores

	B-cl2			P-gp		
	Prop	Intensity	Total	Prop	Intensity	Total
Pre-NACT						
Early LNL Ratio	0.092	0.168	0.162	-0.067	-0.04	-0.059
Delayed LNL Ratio	0.05	-0.118	0.006	-0.14	-0.233	-0.178
Retention Index	-0.223	-0.364*	-0.337#	-0.131	-0.189	-0.156
Post-NACT						
Qualitative scores	0.106	0.141	0.141	-0.474*	-0.229	-0.371
Early LNL Ratio	-0.366	-0.305	-0.394#	-0.406*	-0.315	-0.379
Delayed LNL Ratio	-0.285	-0.199	-0.268	-0.283	-0.088	-0.197
Retention Index	0.167	0.291	0.248	0.275	0.425#	0.364

means marginal significance (P value <0.1 & ≥0.05). * means statistical significance (P value <0.05)

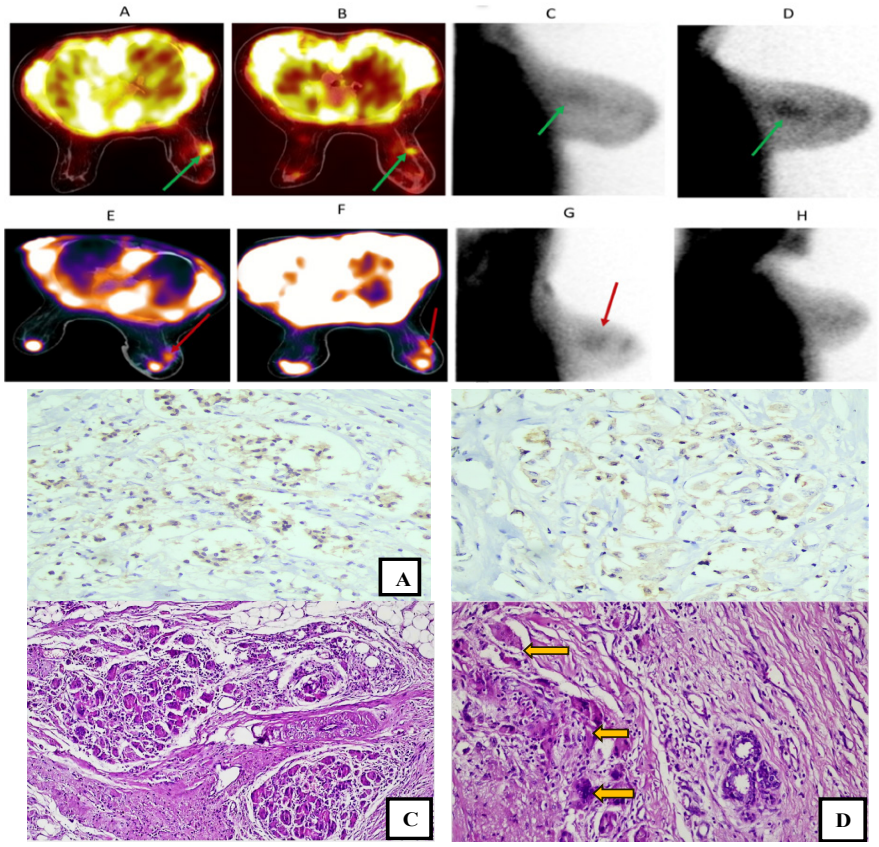

Figure 6. Pre- and Post-NACT Early and Delayed 99mTc-MIBI SPECT/CT and Planar Images of 35-Year-Old Women with Right Sided LABC (A, B, C, D) and (E, F, G, H) respectively. Pre-NACT images (Top row) showed positive tracer uptake in tumor (green arrows), with evidence of metabolically active residual tumor in the post-NACT images (Bottom row, red arrows) suggesting a failed response to NACT. However, post-surgical pathological analysis revealed a complete pathological response, denoting a false positive result. Pre-NACT immunohistochemical profiling of Bcl-2 and P-gp (A&B) revealed: (A) Pre-NACT cytoplasmic low expression of Bcl-2 in (total score 3) (20x magnification). (B) Pre-NACT cytoplasmic low expression of P-gp (total score 3) (40x magnification). (C) Post-NACT tumor bed showed granulomatous reaction formed of chronic inflammation (histiocytes, lymphocytes, foreign body giant cells) (10x magnification) (D) Post-NACT tumor bed showed granulomatous reaction formed of chronic inflammation with numerous foreign body giant cells (yellow arrows) and the adjacent apparently normal breast parenchyma devoids from any tumor tissue (20x magnification).]

Table 5. Univariate Analysis of Patient's Characteristics, SPECT/CT Imaging Metrics and Disease-Free Survival (DFS) and Overall Survival (OS)

Characteristic	3-year OS		3-year DFS	
	HR (95%CI)	P	HR (95%CI)	P
Age (≥50 years)	0.8 (0.2-2.9)	0.78	0.2 (0.1-1.1)	0.067
ypT	1.4 (0.6-3.2)	0.422	3.6 (0.9-14.2)	0.068
ypN	3.8 (1-15)	0.058	1.8 (0.9-3.5)	0.084
PR	4.6 (1-21.8)	0.056	0.9 (0.2-3)	0.803
her2neu	2.2 (0.5-9.2)	0.264	10.2 (2.5-42.5)	0.001*
PNI	5.4 (1.1-27)	0.042*	1.3 (0.4-4.7)	0.66
Post-NACT b-cl2 proportion score (ordinal)	1.5 (0.7-3.2)	0.271	3.2 (1-10.1)	0.048*
post-NACT b-cl2 intensity score (ordinal)	2.7 (1.1-7)	0.036*	1.7 (0.8-3.9)	0.188
Post-NACT b-cl2 total score (ordinal)	1.5 (0.9-2.4)	0.12	1.5 (1-2.5)	0.074
Post-NACT b-cl2 total score (High vs. low)	2.4 (0.3-19.3)	0.425	2.8 (0.3-23)	0.334
Post-NACT P-gp proportion score (ordinal)	1.1 (0.6-2)	0.865	2.4 (1.1-5)	0.020*
Post-NACT P-gp intensity score (ordinal)	1.1 (0.6-2.1)	0.796	2 (1.1-3.8)	0.034*
Post-NACT P-gp total score (ordinal)	1 (0.7-1.5)	0.817	1.6 (1.1-2.3)	0.019*
Post-NACT P-gp total score (High vs. low)	1 (0.2-4.3)	0.975	5.8 (1.1-29)	0.034*
Change in retention index	0.9 (0.8-1.1)	0.404	0.7 (0.6-1)	0.021*

Discussion

MDR to multiple chemotherapeutic agents is a challenging phenomenon in cancer management [28] Thereby, it is important to identify patients who would resist chemotherapy to spare overtreatment with inefficacious chemotherapy. In this context, ^{99m}Tc-MIBI imaging may fulfill the need for fast, non-invasive, simple, and reliable assessment of non-responding patients.

^{99m}Tc-MIBI tissue uptake and retention is ultimately related to cellular metabolic (especially mitochondrial) activity and the expression of MDR associated plasma membrane proteins such as P-gp and the outer mitochondrial membrane Bcl-2 protein, thus its rapid efflux has been considered as an in-vivo indicator of chemoresistance which can provide prognostic information in cases undergoing NACT [29].

Limited spatial resolution of the general-purpose (conventional) gamma cameras was considered the main drawback for breast specific imaging (BSI). However, SPECT imaging added remarkable data and provided a substantial improvement for BSI using such cameras; which are more widely available compared to dedicated breast specific gamma cameras; allowing visualization of the subcentimetric lesions [30].

Regarding qualitative evaluation, a meta-analysis of ^{99m}Tc-MIBI scintimammography for the prediction of pathologic response to NACT, revealed a pooled sensitivity and specificity of 86% and 69% respectively [31].

In the present study, based on pathologic response as the gold standard, SPECT/CT reported sensitivity in detecting residual tumor was marginally higher than planar (P= 0.07). Of 21 patients underwent post-NACT MIBI scintimammography, SPECT/CT successfully demonstrated residual disease in 5 of 8 false negative scans on planar imaging. Three patients were misclassified as negative on SPECT/CT; one of them had post-NACT Bcl-2 score of 7 compared to pre-NACT Bcl-2 score of 0 (Figure 4).

The second case had post-NACT P-gp score of 4 compared to pre-NACT P-gp of 2, both suggesting acquired resistance during chemotherapy, as it accounts for about 50% of cases with chemoresistance [32]. In the third case, surgery was delayed for about 2 months after the end of NACT, disease progression during this time interval may be the attributable factor for non-complete pathological response in this case (Figure 5). It is worth mentioning that residual tumor size, tumor type and differentiation, retained vascularity, as well as the proportion of residual cellularity can have the potential to yield FN findings upon ^{99m}Tc-MIBI scintimammography [33].

On the other hand, a single false positive result was observed in one patient in both planar and SPECT/CT imaging; the postoperative pathologic examination demonstrated a foreign body granuloma (Figure 6). It is well known that inflammatory lesions, as in our case, are one of the important causes of false positive MIBI uptake [34]. Indeed, Park DW et al. in a case report, reported a post-NACT false positive MIBI uptake mimicking residual tumor in a BC patient because of a pathologically-proven foreign body (charcoal) granuloma [35].

These findings are similar to those reported by Spanu et al. who compared planar and SPECT imaging in evaluating response to NACT/hormonal therapy in 32 patients with LABC and demonstrated an identical specificity for both imaging techniques while SPECT yielded a higher sensitivity in assessing the posttherapy residual tumor, but without statistical significance [36].

Bcl-2 gene is involved in cell survival rather than cellular proliferation by preventing apoptosis via activating different signaling pathways [37]. As mentioned above, defective apoptosis likely results in absent or reduced early ^{99m}Tc-MIBI uptake in BC [17].

Concerning quantitative analysis, for pre-NACT Bcl-2, we found a significant negative correlation between pre-NACT Bcl-2 intensity and RI, advocating the effect of Bcl-2 levels on the degree of tracer accumulation in MIBI-positive lesions.

On the other hand, we observed a positive correlation between pre-NACT Bcl-2 expression and early LNL ratios; other factors such as tumor blood flow, viability, and mitochondrial activity were thought to affect the initial ^{99m}Tc-MIBI uptake [38]. This appears to contrast with the results of a previous study which demonstrated a consistent association between lack of ^{99m}Tc-MIBI uptake and pre-NACT Bcl-2 overexpression in ^{99m}Tc-MIBI-negative lesions and a significant negative correlation between early LNL ratios and pre-NACT Bcl-2 levels in ^{99m}Tc-MIBI-positive lesions, indicating that early ^{99m}Tc-MIBI uptake is affected by alterations of apoptotic pathway. The authors suggested that the inhibitory effect of Bcl-2 on the mitochondrial membrane's permeability may provide a possible explanation for their observations [22].

Regarding pre-NACT P-gp, our study revealed a negative, yet insignificant correlation between pre-NACT P-gp expression and RI. Cayre and colleagues reported a significant inverse correlation between pre-NACT MDR1 expression and MIBI accumulation in BC and suggested that ^{99m}Tc-MIBI is a possible indicator of MDR1 chemoresistance [21]. Methodological heterogeneity used to measure MDR and different scintigraphy protocols, in addition, only patients with IDC were enrolled in their evaluation of the correlation between MIBI accumulation and MDR proteins expression could explain the different results.

Also, our study demonstrated a negative correlation between pre-NACT P-gp and both early and delayed LNL ratios. Mubashar et al. found a negative correlation between delayed LNL ratio and pre-NACT P-gp expression [39]. Interestingly, we observed a marginal significant positive correlation between post-NACT P-gp intensity and RI, as well as a positive correlation between post-NACT Bcl-2 scores and RI. We hypothesize that NACT may suppress the metabolic function of the expressed MDR related proteins. However, further studies are required to confirm our hypothesis.

We found that pre-NACT SPECT based RI is insignificantly higher in responders than in non-responders which is in line with what was also reported by Takamura et al. [40] Absence of a significant relation between pre-

NACT RI and chemotherapeutic response may to be attributable, at least in part, to the early LNL component of RI. Early uptake might be affected not only by ^{99m}Tc-MIBI efflux but also by tumor vascularization.

Marshall et al, investigated the chemotherapeutic response in LABC and reported that ^{99m}Tc-MIBI uptake was reduced in 24 of 26 studied patients following NACT [41]. Similar results were obtained by Koga et al, who observed that ^{99m}Tc-MIBI uptake was reduced in almost all of the studied cases of LABC after chemotherapy [42]. Additionally, Reyes et al, observed a good correlation between reduced ^{99m}Tc-MIBI uptake and the response to NACT in LABC [43]. These findings support previous reports demonstrating that the ^{99m}Tc-MIBI uptake reflects cellular metabolism which decreases after chemotherapy [44].

We found a significant association between SPECT-based change in the RI following NACT and DFS (HR = 0.7; 95%CI: 0.6-1; P = 0.021). In this univariate analysis, increasing RI by 1% between pre- and post-NACT, would reduce the likelihood of the disease progressing by 30%. We assume the higher RI in post-NACT scans represent a lower functioning P-gp expression with higher potential for substrate retention, which includes chemotherapies, and accordingly lead to better response.

Chemoresistance and metastasis in some BC molecular subtypes, especially in TNBC, are still inevitable and lead to poor prognosis [45] The current research documented that high post-NACT Bcl-2 was significantly associated with Luminal A and Her2 enriched types while low expression was significantly associated with TNBC. This finding aligned with Honma et al. study which noted that Bcl-2 positivity was significantly correlated with ER and PR positivity. However, in contrast to ours in cases of Her2 enriched subtype. (46) The favorable prognosis previously associated with Bcl-2-positive BC probably reflects the indirect effect of frequently expressed hormone receptors and adjuvant endocrine therapy [46].

In our study, post-NACT Bcl-2 high expression was significantly associated with advanced tumor stage while no significant result with pre-NACT Bcl-2. This is disagreed with Honma et al. study which noted Bcl-2 expression was strongly correlated with small tumor size [46]. This discrepancy may be attributed to different study populations and treatment modality as we examined Bcl-2 expression in both pre- and post-NACT specimens in the same cases while Honma et al. compared Bcl-2 expression among different patient groups; with the first group did not receive any adjuvant therapy and the other group received adjuvant tamoxifen monotherapy.

P-gp counteract the intracellular load of multiple drugs, [28] via efflux of chemotherapeutic agents, subsequently reducing its cellular accumulation and toxicity. As a result, chemotherapeutic efficacy is decreased. Inhibiting P-gp activity with effective and non-toxic products is promising [47]. PPD was significantly associated with high expression post-NACT P-gp in the current research. Additionally, post-NACT P-gp high expression in our study showed significant relation with the presence of LVI and LNM. MDR phenotype is associated with elevated invasion and metastasis of tumor cells [48]. P-gp is one of the main determinants in MDR phenotype generation and an aggressive phenotype and associated with poor prognosis in various malignancies. The invasive potential of MDR BC cells will be enhanced by P-gp, by modulating the tyrosine phosphorylation of ANXA2. So, the interaction between ANXA2 and P-gp is possibly responsible for the association between MDR and invasive potential in BC cells [48].

A substantial positive correlation was demonstrated between Pre-NACT P-gp and Bcl-2 scores in the present research. Volger et al. documented Bcl-2 inhibitors like ABT-737 and ABT-263 are substrates for P-gp. Overexpression of P-gp may be responsible for resistance to these Bcl-2 inhibitors that evade apoptosis [49].

We found that higher post-operative Bcl-2 expression and advanced LNM were significantly associated with poor OS. This aligns with the previous finding by Ozretic et al., which suggested that patients exhibiting high Bcl-2 expression experienced a shorter OS. The same was observed for patients with positive lymph nodes [50]. Unlike our results, an earlier study documented that Bcl-2 negativity was associated with a shorter OS.26 The variation between the results may be due to differences in the study designs.

The current study demonstrated a significantly worse impact of higher post-NACT P-gp on DFS. This is in disagreement with Prajoko et al. who found that expression of P-gp had no significant role in metastases, recurrence, or survival in patients who received NACT [51].

There were some limitations in our study. First, it was a single center study. Second, due to the COVID-19 pandemic, we were unable to do post-NACT scans for all patients who underwent surgery. A global assessment on COVID-19's impact on nuclear medicine services found a significant decrease in diagnostic and therapeutic nuclear medicine activities by more than 50% and up to 45%, respectively [52]. Third, a multivariable analysis could not be performed and modeling the interaction between the different covariates was not possible.

This preliminary study provides grounds for conducting further prospective, thorough, and long-term studies, taking into consideration that it includes multicenter collaborative working group and larger patient samples to verify our results.

In conclusion, we found that the sensitivity of ^{99m}Tc-MIBI SPECT/CT was more sensitive than planar imaging in qualitative evaluation of BC response to NACT, that SPECT-based pre-NACT ^{99m}Tc-MIBI retention was higher in NACT responders, albeit insignificantly, and that change in ^{99m}Tc-MIBI RI between pre- and post-NACT studies is significantly associated with improved DFS. Also, we documented a positive correlation between the investigated MDR related proteins and RI in the post-NACT setting, suggesting that NACT has a suppressive effect on their metabolic activity. We hypothesize that ^{99m}Tc-MIBI SPECT/CT functional imaging may predict MDR development.

Our data revealed a significant association between high post-NACT Bcl-2 expression, and advanced tumor stage and poor OS, as well as a significant worse impact of the high post-NACT P-gp expression on pathologic

response and DFS.

Author Contribution Statement

Study concepts: NM, MS, YG, KR, MF, HA, SA, MT. Study design: NM, MS, YG, KR, MF, HA, SA, MT.

Data acquisition: NM, MS, YG, HA, MT. Data analysis and interpretation: NM, YG, HA, MT. Statistical analysis: YG, MT. Manuscript preparation: NM, YG, HA, MT. Manuscript editing: NM, YG, HA, MT. Manuscript review: NM, MT.All authors read and approved the final manuscript

Acknowledgements

Funding statement

This research received fund from Assiut University.

Approval

This study was performed in line with the principles of the Declaration of Helsinki. Approval was granted by the Ethics Committee of SECI, Assiut University, Egypt, with IRB number IORG0006563.

Availability of data (if apply to your research)

The datasets used and analyzed during the current study are available from the corresponding author on reasonable request.

Conflict of interest

None.

References

1. Bray F, Ferlay J, Soerjomataram I, Siegel RL, Torre LA, Jemal A. Global cancer statistics 2018: GLOBOCAN estimates of incidence and mortality worldwide for 36 cancers in 185 countries. CA Cancer J Clin. 2018;68(6):394–424. https://doi.org/10.3322/caac.21492.
2. Amin MB, Greene FL, Edge SB, Compton CC, Gershenwald JE, Brookland RK, et al. The eighth edition AJCC cancer staging manual: continuing to build a bridge from a population-based to a more "personalized" approach to cancer staging. CA: Cancer J Clin. 2017;67(2):93-9. https://doi.org/10.3322/caac.21388
3. Semiglazov VF, Semiglazov VV, Paltuev RM, Dashyan GA, Semiglazova TY, Krivorotko P V, et al. Neoadjuvant treatment for breast cancer. Tumors female Reprod Syst. 2014;(2):30–6. https://doi.org/10.17650/1994-4098-2014-0-2-30-36.
4. Bukowski K, Kciuk M, Kontek R. Mechanisms of multidrug resistance in cancer chemotherapy. Int J Mol Sci. 2020;21(9):3233. https://doi.org/10.3390/ijms21093233.
5. Colomer R, Saura C, Sánchez-Rovira P, Pascual T, Rubio IT, Burgués O, et al. Neoadjuvant management of early breast cancer: a clinical and investigational position statement. Oncologist. 2019;24(5):603. https://doi.org/10.1634/theoncologist.2018-0228.
6. Mansoori B, Mohammadi A, Davudian S, Shirjang S, Baradaran B. The different mechanisms of cancer drug resistance: a brief review. Adv Pharm Bull. 2017;7(3):339. https://doi.org/10.15171/apb.2017.041.
7. He J, Fortunati E, Liu DX, Li Y. Pleiotropic Roles of ABC Transporters in Breast Cancer. Int J Mol Sci. 2021;22(6):3199. https://doi.org/10.3390/ijms22063199.
8. Marin JJG, Al-Abdulla R, Lozano E, Briz O, Bujanda L, M Banales J, et al. Mechanisms of resistance to chemotherapy in gastric cancer. Anti-Cancer Agents Med Chem (Formerly Curr Med Chem Agents). 2016;16(3):318–34. https://doi.org/10.2174/1871520615666150803125121.
9. Majidinia M, Mirza-Aghazadeh-Attari M, Rahimi M, Mihanfar A, Karimian A, Safa A, et al. Overcoming multidrug resistance in cancer: Recent progress in nanotechnology and new horizons. IUBMB Life. 2020;72(5):855–71. https://doi.org/10.1002/iub.2215.
10. Dizdarevic S, Peters AM. Imaging of multidrug resistance in cancer. Cancer Imaging. 2011;11(1):1. https://doi.org/10.1102/1470-7330.2011.0001.
11. Nanayakkara AK, Follit CA, Chen G, Williams NS, Vogel PD, Wise JG. Targeted inhibitors of P-glycoprotein increase chemotherapeutic-induced mortality of multidrug resistant tumor cells. Sci Rep. 2018;8(1):1–18. https://doi.org/10.1038/s41598-018-19325-x.
12. Wolking S, Schaeffeler E, Lerche H, Schwab M, Nies AT. Impact of genetic polymorphisms of ABCB1 (MDR1, P-glycoprotein) on drug disposition and potential clinical implications: update of the literature. Clin Pharmacokinet. 2015;54(7):709–35. https://doi.org/10.1007/s40262-015-0267-1
13. Clarke R, Leonessa F, Trock B. Multidrug resistance/P-glycoprotein and breast cancer: review and meta-analysis. In: Seminars in oncology. Elsevier. 2005;32(6 Suppl 7):9–15. https://doi.org/10.1053/j.seminoncol.2005.09.009.
14. Piwnica-Worms D, Kesarwala AH, Pichler A, Prior JL, Sharma V. Single photon emission computed tomography and positron emission tomography imaging of multi-drug resistant P-glycoprotein—monitoring a transport activity important in cancer, blood–brain barrier function and Alzheimer's disease. Neuroimaging Clin. 2006;16(4):575–89. https://doi.org/10.1016/j.nic.2006.06.007.
15. Bigott HM, Prior JL, Piwnica-Worms DR, Welch MJ. Imaging multidrug resistance P-glycoprotein transport function using microPET with technetium-94m-sestamibi. Mol Imaging. 2005;4(1):15353500200504166. https://doi.org/10.1162/15353500200504166.
16. Del Vecchio S, Ciarmiello A, Salvatore M. Scintigraphic detection of multidrug resistance in cancer. Cancer Biother Radiopharm. 2000;15(4):327–37. https://doi.org/10.1089/cbr.2000.15.327.
17. Vecchio S Del, Zannetti A, Salvatore B, Paone G, Fonti R, Salvatore M. Functional imaging of multidrug resistance in breast cancer. Phys Med. 2006;21:24–7. https://doi.org/10.1016/S1120-1797(06)80019-0.
18. Moretti JL, Hauet N, Caglar M, Rebillard O, Burak Z. To use MIBI or not to use MIBI? That is the question when assessing tumour cells. Eur J Nucl Med Mol Imaging. 2005;32(7):836–42. https://doi.org/10.1007/s00259-005-1840-x.
19. Del Vecchio S, Ciarmiello A, Pace L, Potena MI, Carriero MV, Mainolfi C, et al. Fractional retention of technetium-^{99m}-sestamibi as an index of P-glycoprotein expression in untreated breast cancer patients. J Nucl Med. 1997;38(9):1348–51.
20. Vecchio SD, Ciarmiello A, Potena MI, Carriero MV, Mainolfi C, Mainolfi C. In vivo detection of multidrug-resistant (MDR1) phenotype by technetium-^{99m} sestamibi scan in untreated breast cancer patients. Eur J Nucl Med. 1997;24:150–9. https://doi.org/10.1007/BF02439547.
21. Cayre A, Cachin F, Maublant J, Mestas D, Feillel V, Ferriere JP, et al. Single static view ^{99m}Tc-sestamibi scintimammography predicts response to neoadjuvant chemotherapy and is related to MDR expression. Int J Oncol.

2002;20(5):1049–55. https://doi.org/10.3892/ijo.20.5.1049.
22. Del Vecchio S, Zannetti A, Aloj L, Caracò C, Ciarmiello A, Salvatore M. Inhibition of early ^{99m} Tc-MIBI uptake by Bcl-2 anti-apoptotic protein overexpression in untreated breast carcinoma. Eur J Nucl Med Mol Imaging. 2003;30:879–87. https://doi.org/10.1007/s00259-003-1161-x.
23. Oken MM, Creech RH, Tormey DC, Horton J, Davis TE, McFadden ET, et al. Toxicity and response criteria of the Eastern Cooperative Oncology Group. Am J Clin Oncol. 1982;5(6):649–56.
24. Eisenhauer EA, Therasse P, Bogaerts J, Schwartz LH, Sargent D, Ford R, et al. New response evaluation criteria in solid tumours: revised RECIST guideline (version 1.1). Eur J Cancer. 2009;45(2):228–47. https://doi.org/10.1016/j.ejca.2008.10.026.
25. Larkin A, O'Driscoll L, Kennedy S, Purcell R, Moran E, Crown J, et al. Investigation of MRP-1 protein and MDR-1 P-glycoprotein expression in invasive breast cancer: A prognostic study. Int J cancer. 2004;112(2):286–94. https://doi.org/10.1002/ijc.20369.
26. Čečka F, Hornychová H, Melichar B, Ryška A, Jandík P, Mergancová J, et al. Expression of bcl-2 in breast cancer: correlation with clinicopathological characteristics and survival. Acta Medica (Hradec Kral Czech Republic). 2008;51(2):107–12. https://doi.org/10.14712/18059694.2017.11.
27. Brem RF, Floerke AC, Rapelyea JA, Teal C, Kelly T, Mathur V. Breast-specific gamma imaging as an adjunct imaging modality for the diagnosis of breast cancer. Radiology. 2008;247(3):651–7. https://doi.org/10.1148/radiol.2473061678.
28. Levi M, Muscatello LV, Brunetti B, Benazzi C, Parenti F, Gobbo F, et al. High intrinsic expression of P-glycoprotein and breast cancer resistance protein in canine mammary carcinomas regardless of immunophenotype and outcome. Animals. 2021;11(3):658. https://doi.org/10.3390/ani11030658.
29. Marín-Rodríguez P, Ruiz-Merino G, Castellón-Sánchez M, Iborra-Lacal E, Marín-Hernández C, Navarro-Fernández JL, et al. Is the result of breast Tc-^{99m} mibi scintigraphy a prognostic factor for survival in invasive breast cancer? Rev Senol y Patol Mamar. 2021;34(1):23–9. https://doi.org/10.1016/j.senol.2020.05.002.
30. Azarpeikan AR, Omranipour R, Mahmoodzadeh H, Miri SR, Mohammadzadeh N, Derakhshan F, et al. Application of breast scintigraphy for patients with suspicious (breast imaging-reporting and data system IV) breast lesions. Adv Biomed Res. 2023;12. https://doi.org/10.4103/abr.abr_347_21.
31. Guo C, Zhang C, Liu J, Tong L, Huang G. Is Tc-^{99m} sestamibi scintimammography useful in the prediction of neoadjuvant chemotherapy responses in breast cancer? A systematic review and meta-analysis. Nucl Med Commun. 2016;37(7):675–88. DOI: 10.1097/MNM.0000000000000502.
32. Wang X, Zhang H, Chen X. Drug resistance and combating drug resistance in cancer. Cancer Drug Resist. 2019;2(2):141. https://doi.org/10.20517/cdr.2019.10.
33. Sampalis FS, Denis R, Picard D, Fleiszer D, Martin G, Nassif E, et al. International prospective evaluation of scintimammography with ^{99m}Technetium sestamibi. Am J Surg. 2003;185(6):544–9. https://doi.org/10.1016/S0002-9610(03)00077-1.
34. Goldsmith SJ, Parsons W, Guiberteau MJ, Stern LH, Lanzkowsky L, Weigert J, et al. SNM practice guideline for breast scintigraphy with breast-specific γ-cameras 1.0. J Nucl Med Technol. 2010;38(4):219–24. https://doi.org/10.2967/jnmt.110.082271.
35. Park DW, Park JY, Park NH, Kim SJ, Shin HJ, Lee JJ, et al. A Case of Recurrence-Mimicking Charcoal Granuloma in a Breast Cancer Patient: Ultrasound, CT, PET/CT and Breast-Specific Gamma Imaging Findings. J Korean Soc Radiol. 2016;75(1):57–61. https://doi.org/10.3348/jksr.2016.75.1.57.
36. Spanu A, Farris A, Chessa F, Sanna D, Pittalis M, Manca A, et al. Planar scintimammography and SPECT in neoadjuvant chemo or hormonotherapy response evaluation in locally advanced primary breast cancer. Int J Oncol. 2008;32(6):1275–83. https://doi.org/10.3892/ijo_32_6_1275.
37. Berrak Ö, Akkoç Y, Arısan ED, Çoker-Gürkan A, Obakan-Yerlikaya P, Palavan-Ünsal N. The inhibition of PI3K and NFκB promoted curcumin-induced cell cycle arrest at G2/M via altering polyamine metabolism in Bcl-2 overexpressing MCF-7 breast cancer cells. Biomed Pharmacother. 2016;77:150–60. https://doi.org/10.1016/j.biopha.2015.12.007.
38. Omer WS, Elasa S, Mouslafa H, Farag H, Ezzat I, Abdel-Dayam HM. Role of thallium-201 and Tc-^{99m}-methoxy-iosobutylisonitril (sestamibi) in evaluation of breast masses: correlation with immunohistochemical characteristic parameters (ki-67, PCNA, Bcl-2 and antiangiogenesis) in malignant lesions. Anticancer Res. 1997;17:1639–44.
39. Mubashar M, Harrington KJ, Chaudhary KS, Lalani EN, Stamp GW, Sinnett D, et al. ^{99m}Tc-sestamibi imaging in the assessment of toremifene as a modulator of multidrug resistance in patients with breast cancer. J Nucl Med. 2002;43(4):519–25.
40. Takamura Y, Miyoshi Y, Taguchi T, Noguchi S. Prediction of chemotherapeutic response by Technetium ^{99m}–MIBI scintigraphy in breast carcinoma patients. Cancer Interdiscip Int J Am Cancer Soc. 2001;92(2):232–9. https://doi.org/10.1002/1097-0142(20010715)92:2<232::aid-cncr1314>3.0.co;2-g.
41. Marshall C, Eremin J, El-Sheemy M, Eremin O, Griffiths PA. Monitoring the response of large (> 3 cm) and locally advanced (T3–4, N0–2) breast cancer to neoadjuvant chemotherapy using ^{99m}Tc-Sestamibi uptake. Nucl Med Commun. 2005;26(1):9–15. https://doi.org/10.1097/00006231-200501000-00003.
42. Koga KH, Moriguchi SM, Nahás Neto J, Verzinhasse Peres S, Tinóis Da Silva E, Sarri AJ, et al. ^{99m}Tc-sestamibi scintigraphy used to evaluate tumor response to neoadjuvant chemotherapy in locally advanced breast cancer: A quantitative analysis. Oncol Lett. 2010;1(2):379–82. https://doi.org/10.3892/ol_00000067.
43. Reyes R, Parbhoo SP, Cwikla JB, Buscombe JR, Jones AL, Hilson AJW. The role of scintimammography in prediction of response to primary chemotherapy. Eur J Cancer. 2000;36:S136.
44. Lastoria S, Varella P, Thomas R, D'Aiuto G, Acampa W, Vergara E. Predicting and monitoring the treatment in breast cancer by scintimammography with Tc-99 m MIBI. J Nucl Med. 1996;37:156P.
45. Nikolaou M, Pavlopoulou A, Georgakilas AG, Kyrodimos E. The challenge of drug resistance in cancer treatment: a current overview. Clin Exp Metastasis. 2018;35:309–18. https://doi.org/10.1007/s10585-018-9903-0.
46. Honma N, Horii R, Ito Y, Saji S, Younes M, Iwase T, et al. Differences in clinical importance of Bcl-2 in breast cancer according to hormone receptors status or adjuvant endocrine therapy. BMC Cancer. 2015;15:1–11. https://doi.org/10.1186/s12885-015-1686-y.
47. Abd-Ellatef GEF, Gazzano E, El-Desoky AH, Hamed AR, Kopecka J, Belisario DC, et al. Glabratephrin reverses

doxorubicin resistance in triple negative breast cancer by inhibiting P-glycoprotein. Pharmacol Res. 2022;175:105975. https://doi.org/10.1016/j.phrs.2021.105975.
48. Yang Y, Wu N, Wang Z, Zhang F, Tian R, Ji W, et al. Rack1 mediates the interaction of P-glycoprotein with Anxa2 and regulates migration and invasion of multidrug-resistant breast cancer cells. Int J Mol Sci. 2016;17(10):1718. https://doi.org/10.3390/ijms17101718.
49. Vogler M, Dickens D, Dyer MJS, Owen A, Pirmohamed M, Cohen GM. The B-cell lymphoma 2 (BCL2)-inhibitors, ABT-737 and ABT-263, are substrates for P-glycoprotein. Biochem Biophys Res Commun. 2011;408(2):344–9. https://doi.org/10.1016/j.bbrc.2011.04.043.
50. Ozretic P, Alvir I, Sarcevic B, Vujaskovic Z, Rendic-Miocevic Z, Roguljic A, et al. Apoptosis regulator Bcl-2 is an independent prognostic marker for worse overall survival in triple-negative breast cancer patients. Int J Biol Markers. 2018;33(1):109–15. https://doi.org/10.5301/ijbm.5000291.
51. Prajoko YW, Aryandono T. The effect of p-glycoprotein (P-gp), nuclear factor-kappa B (Nf-κb), and aldehyde dehydrogenase-1 (ALDH-1) expression on metastases, recurrence and survival in advanced breast cancer patients. Asian Pac J Cancer Prev. 2019;20(5):1511. https://doi.org/10.31557/APJCP.2019.20.5.1511.
52. Al-Saeedi F, Rajendran P, Tipre D, Aladwani H, Alenezi S, Alqabandi M, et al. The effect of COVID-19 on nuclear medicine and radiopharmacy activities: A global survey. Sci Rep. 2023;13(1):10489. https://doi.org/10.1038/s41598-023-36925-4.